



Dielectric Properties of Butyl rubber/graphite powder composites in bulk and membrane forms

M. Amin, G. M. Nasr, G. H. Ramzy*, E. Omar.

^a Physics department, Faculty of science, Cairo University, Giza, Egypt

Received 18 Feb 2013, Revised 5 Apr 2013, Accepted 5 Apr 2013

*Corresponding author: galalramzy@yahoo.com, Mobile number: +201002798656

Abstract

Samples of butyl rubber(IIR)/ graphite powder were prepared using two different methods in bulk and membrane forms. The dielectric properties were studied in the frequency range $10^2 - 2 \times 10^5$ Hz. The behavior of the dielectric constant and the AC conductivity were found to be described by the well-known percolation theory. The percolation threshold for both types of samples was found to be around 0.25. A deviation in the value of the percolation exponent from the universal value was found and this also was explained.

Keywords: dielectric properties, IIR, graphite, percolation.

Introduction

Conducting polymer composites (CPC) have become the subject of an increased research interest [1-5] due to their great variety of applications such as electroluminescence, sensors and energy storage systems. In order to get a satisfactory conductivity level, using conventional graphite powder fillers, polymer composites loadings need to be about 20 wt% or even higher. However, high graphite powder filler concentration could always lead to not only materials redundancy and detrimental mechanical properties but also a high threshold value (the percolation threshold) [1, 6, 7]. Celzard *et al.* [8] reported an epoxy/expanded graphite (E.G) composites with a percolation threshold of 1.3 vol.% of E.G fillers by subjecting the graphite powder to a rapid thermal treatment. Recently, several groups reported PMMA/E.G, PS/PG, PS/PMMA/E.G composites with markedly low threshold values [9–14]. Efimov and coworkers [15] and Meng and coworkers [16] also researched the conductivity of PANI/ graphite composites, but the graphite was natural expandable graphite, and the size was at micrometer and millimeter scales. At the basis of these experiments, Chen *et al.* [17] revealed that the graphite nanosheets (NanoG) were prepared by E.G with ultrasonic irradiation. The NanoG is nanosized (with thickness of 30–80 nm and diameter of 5–20 μ m) and the high aspect ratio (diameter to thickness), about 100–300. More recently, NanoG was used to prepare PS/NanoG [18] and PMMA/NanoG [19] composites with very low values of percolation threshold, about 1.6 and 1.5 vol%, respectively.

The aim of the present work is to study the influence of the varying the final shape and the method of preparation on the dielectric properties of IIR/graphite powder composites.

2. Materials and methods

2.1. Materials used in this Work

Butyl rubber (IIR) was supplied by TRENCO, Alexandria, Egypt and the fine powder extra pure graphite (50 μ m) was supplied by Merck, Germany were used in this study. Graphite properties are: Solubility (20 $^{\circ}$ C) insoluble; Molar mass 12.01 g/mol; Density 2.2 g/cm³ (20 $^{\circ}$ C); Bulk density 280 kg/m³; pH value 5 - 6 (50 g/l, H₂O, 20 $^{\circ}$ C). The calculation of the true graphite volume fraction was performed through the following relationship:

$$\varphi_{\text{true graphite}} = \frac{w_{\text{true graphite}} / \rho_{\text{true graphite}}}{\sum_i w_i / \rho_i} \quad (1)$$

Where w_i and ρ_i are the weight fraction and the density of the i^{th} phase, respectively.

2.2. Sample preparation and Measurements

2.2.1 Bulk Forms

All samples were prepared according to the following method with the compositions shown in table (1). Ingredients of the rubber composites were mixed on a 2-roll mill of 170 mm diameter, working distance 300-

mm, speed of slow roll being 24 rpm and gear ratio 1.4. The compounded rubber was divided into two groups; the first group was left for 24 hours before vulcanization. The vulcanization process was performed at $153 \pm 2^\circ\text{C}$ under a pressure of 150 bar for 15 minutes. To ensure reproducibility of the results, the samples were aged at 70°C for 10 days. By this way the bulky samples were prepared with average thickness 0.3 cm.

2.2.2 Membrane Form

This group was prepared by dissolving the second group in methylbenzene to obtain a highly concentrated solution. Subsequently, each gelatinous solution was shaped into membrane in a form of circle (7 cm in diameter) by means of a stainless steel dish. After slow drying, a smooth and uniform thin composite membrane was obtained about 0.7 mm in thickness. Then all membrane samples were vulcanized under pressure of 294 bar, at temperature 153°C , and time of 30 minutes, the final membranes have average thickness 0.2 mm. Finally they were aged at 70°C for 10 days to insure reproducibility of results.

2.2.3 Measurements and Calculations

The dielectric properties were measured using a bridge (type GM Instek LCR – 821 meter) in the frequency range 10^2 - 10^5 Hz. Both samples capacitance and $\tan \delta$ values were measured for all samples at different temperatures and frequencies. The dielectric constant ϵ' (real part of the complex dielectric constant) of the samples was calculated by using the relation.

$$\epsilon' = \frac{d}{\epsilon_0 A} C \quad (2)$$

Where C is the capacitance of the sample, d is the thickness of the sample, A is the cross-sectional area of each of the parallel surfaces of the sample, and ϵ_0 is the permittivity of free space.

Conducting polymer composites possess a frequency (ω) dependent complex dielectric constant $\epsilon^*(\omega) = \epsilon'(\omega) - i\epsilon''(\omega)$. The real part $\epsilon'(\omega)$ represents the dielectric constant and the imaginary part $\epsilon''(\omega)$ accounts for the dielectric loss. The ratio of the imaginary to the real part (ϵ''/ϵ') is the "dissipation factor" which is denoted by $\tan \delta$, where δ is called the "loss angle" denoting the phase difference between the voltage and the charging current. The AC conductivity can be deduced from the equation $\sigma_{AC} = 2\pi f \epsilon_0 \epsilon''$, where f is the frequency. The dielectric loss ϵ'' is calculated from the equation $\epsilon'' = \epsilon' \tan \delta$.

3. Results and discussion

3.1 Graphite content dependence

The dependence of the dielectric constant ϵ' on the graphite volume fraction ϕ at 100 kHz of the graphite/IIR both in bulk and membrane forms respectively are shown in Figures (1) and (2). The dielectric constant increases moderately up to a point in the vicinity of the percolation threshold obtained from conductivity measurements ($\phi_c \approx 0.25$). Above this point, the dielectric constant increases at a faster rate and exhibits an abrupt change. This increase in the value of the dielectric constant may be attributed to the buildup of space charges at the interface separating the conducting phase and the insulating phase due to the difference in the conductivities of the two phases. This buildup process is referred to as Maxwell-Wagner polarization originating in the insulator-conductor interfaces [20]. Space charge polarization occurs when more than one component is present or when segregation occurs in a material that contains incompatible chemical species and mobile charge carriers are trapped at the interfaces of these heterogeneous systems. The electric field distortion caused by these trapped charges increases the overall capacitance and hence the dielectric constant of the system [21]. However, this enhancement of the dielectric constant in the neighborhood of the percolation threshold ($\phi_c \approx 0.25$) is also predicted by the power law [22-23] as follows:

$$\epsilon' \propto (\phi_c - \phi)^{-t} \quad (3)$$

Where t is a critical exponent. The log-log plots of equation (3) are shown in the inset of Figures (1) & (2). The best fit of the dielectric constant data to the log-log plot of Eq. (3) gives $\phi_c = 0.25$ for IIR/graphite in both bulk and membrane forms. The value of t was found to be 0.24 and 0.048 for IIR/graphite in bulk and membrane forms respectively, which is too small compared to the universal value given by the percolation theory [24]. The reason for the deviation of t from the universal value (~ 2) has also been reported by previous research articles [25-27]. It was reported [25-26] that the theoretical model did not consider the interaction between the conducting particle and the polymer matrix. They concluded that theoretically if physical contact is not necessary (i.e., charges can tunnel through the barrier) to make the percolative network, non-universal value of t

could be obtained for composite systems. Research article [27] reported that the value of t depends on type of simulation used to fit Eq. (3). The best linear fitting to Eq. (3) is obtained by varying the value of φ_c and different values of t are obtained. Also, it has been demonstrated that very high values of t tend to occur when the conducting particles have extreme geometry [28], presence of tunneling conduction can also lead to non-universal critical exponent [28].

3.2 Frequency dependence

The dependence of ϵ' on the frequency for IIR/graphite composites both in the bulk and membrane forms are shown in Figures (3) & (4). The ϵ' of the composites having $\varphi \leq 0.29$ exhibit weak frequency dependence (for bulk and membrane forms), but when $\varphi \geq 0.35$, the ϵ' of the composites exhibits strong dependence and decreases sharply in the frequency range 10^2 Hz to 10^4 Hz, which may be attributed to the large leakage current resulting from the high conductivity composites (except IIR samples in the membrane form which has low conductivity value). At low frequency, a high value of ϵ' of IIR composites with $\varphi \geq 0.35$ was observed because at low frequency, the polarization follows the change of the electric field, and dielectric loss is minimum and hence the contribution to the dielectric constant is maximal. At high frequencies, the electric field changes too fast for the polarization effects to appear. In this case, ϵ' has minimum contribution and there is approximately no dielectric losses in the polymer matrix [29]. A high value of ϵ' is very good in capacitor applications.

Figures (5) & (6) show the frequency dependence of AC electrical conductivity of all samples in bulk and membrane forms respectively. The plot of $\log [\sigma_{AC}(\omega)]$ versus $\log \omega$ emphasizes generally two regimes; a frequency independent plateau and frequency dependent region separated by a critical frequency. The critical frequency depends on the concentration of the filler in the polymer matrix. As the concentration increases, the critical frequency moves toward higher values. To explain this behavior, one can use the universal power law relation [30]

$$\sigma_{AC} = \sigma_{DC} + A\omega^s \quad (4)$$

where σ_{DC} is DC conductivity, A is a temperature-dependent constant, $\omega = 2\pi f$, and s is the frequency exponent ($s \leq 1.0$). However, if the DC conductivity of the composite is very small then the σ_{DC} term can be neglected and the above relation converts to

$$\sigma_{AC} = A\omega^s \quad (5)$$

The exponent s is seen to be a function of ω . We determine the s value, as a function of ω (following Bhattacharyya *et al* method [31] from the slope of the $\log \sigma_{ac}(\omega) - \log(\omega)$ curve at different frequencies for various samples. To obtain the s value, we fitted the $\log \sigma_{ac}(\omega) - \log(\omega)$ data by a polynomial of the form:

$$\log \sigma_{ac}(\omega) = a + b \log \omega + c (\log \omega)^2 \quad (6)$$

The slope at any frequency ω was obtained from the equation [13]

$$s = \frac{d(\log \sigma)}{d(\log \omega)} \quad (7)$$

using equation (6), we obtain

$$s = b + 2c \log \omega \quad (8)$$

In Figures (7) and (8) the variation of s as a function of $\log \omega$ for different samples is shown.

Other models can be used to describe the conduction mechanism and to explain the behaviour of σ_{AC} with both temperature and frequency by using Eq.(5); the first one is the correlated barrier hopping (CBH) model, which was proposed by Elliott [22,32]; another is the quantum mechanical tunnelling (QMT) model, which was proposed by Pollak and Geballe [33] and Austin and Mott [16]. According to the QMT model, the value of the frequency exponent s , which is calculated from the slope of the straight line relating frequency to conductivity, is predicted to be temperature independent but frequency dependent, whereas in the case of the CBH model it is predicted to be temperature and frequency dependent. This regime is attributed to hopping conduction and at enough high frequency the conductivity is higher than the conductivity due to band conduction. The two regimes are clearly visible for samples loaded with graphite < 50 phr and hopping conduction sets in at temperatures greater than 80°C (for samples loaded with graphite ≥ 60 phr) as seen in Figures (5) & (6).

For QMT of electrons, the real part of the AC conductivity within the pair approximation is given by

$$\sigma(\omega) = \frac{\pi^4}{24} e^2 kT \alpha^{-1} [N(E_f)]^2 \omega R^4 \quad (9)$$

where $N(E_f)$ is the density of states at the Fermi level, α^{-1} is the spatial decay parameter for the localized wave function, and R_ω is the tunneling length at frequency ω :

$$R_\omega = (2\alpha)^{-1} \ln \left(\frac{1}{\omega\tau_0} \right) \quad (10)$$

where τ_0 is a characteristic relaxation time. The frequency exponent s in this model is deduced to be:

$$s = 1 + \frac{4}{\ln \left(\frac{1}{\omega\tau_0} \right)} \quad (11)$$

Thus, for QMT of electrons, $\sigma(\omega)$ is linearly dependent on temperature and s is temperature-independent. The correlated barrier hopping (CBH) model was first proposed by Pike[35] to account for ac conduction in amorphous scandium oxide films; it was assumed that single electron motion was responsible. The ac conductivity in this model is expressed by:

$$\sigma(\omega) = \frac{\pi^3}{24} N^2 \varepsilon \varepsilon_0 \omega R_\omega^6 \quad (12)$$

Where N is the density of a pair of sites. The hopping length R_ω is given by:

$$R_\omega = \frac{e^2}{\pi \varepsilon \varepsilon_0} \left[W_m - kT \ln \left(\frac{1}{\omega\tau_0} \right) \right] \quad (13)$$

where W_m is the maximum barrier height. The frequency exponent s in the electron CBH model is evaluated to be:

$$s = 1 + \frac{6kT}{\left[W_m - kT \ln \left(\frac{1}{\omega\tau_0} \right) \right]} \quad (14)$$

It is evident from Figures(7) and (8) that the frequency exponent s decreases with the increase in frequency for samples 20 and 40phr in bulk form and for samples 60,100phr in membrane state. This suggests that the variation follows Eq.(11), indicating a QMT mechanism is operative in these systems. Meanwhile, all other samples show an increase in s as the frequency increase. This is consistent with Eq.(14), indicating the presence of a CBH mechanism. The value of τ_0 for all samples exhibiting a QMT mechanism are summarized in table(2)

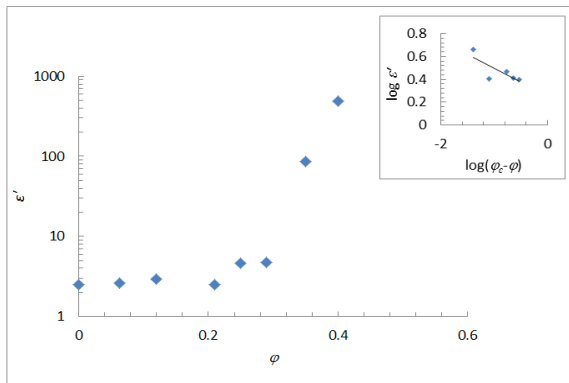
Table (1) Formulation of the rubber compounds

Ingredients		Quantity(phr ^a)
Rubber	IIR	100
Filler	Graphite	0,10,20,30,40,50,60,80,100
Plasticizer	Processing oil	10
Activators	Stearic acid	1.5
	Zinc oxide	5
Accelerator	MBTS ^b	1.5
Age resisters	PBN ^c	1
Vulcanizing Agents	Sulfur	2

^a Parts per hundred parts by weight of rubber

Table (2): Values of relaxation time τ_0 for all samples exhibiting a QMT mechanism

	Graphite content(phr)	τ_0 (s)
IIR bulk	20	10
	40	10 ³
IIR membrane	60	10 ⁻²²
	100	10 ⁻¹⁸



Figure(1): shows the variation of ϵ' of graphite/IIR in bulk form as a function of graphite volume fraction at 100 kHz

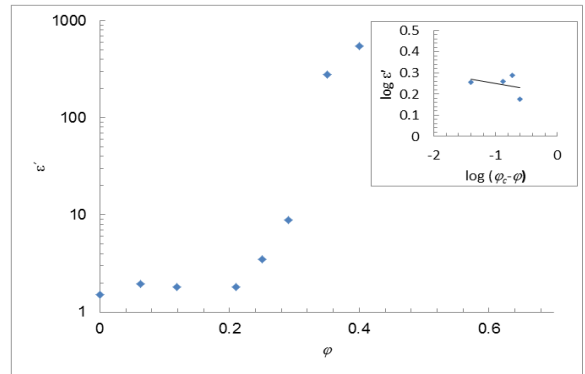


Figure 2: shows the variation of ϵ'' of graphite/IIR membrane form as a function of graphite volume fraction at 100 kHz

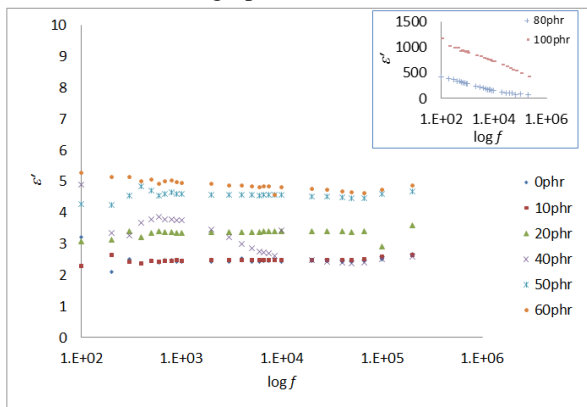


Figure (3): Frequency dependence of ϵ' of IIR/graphite composites in the bulk form.

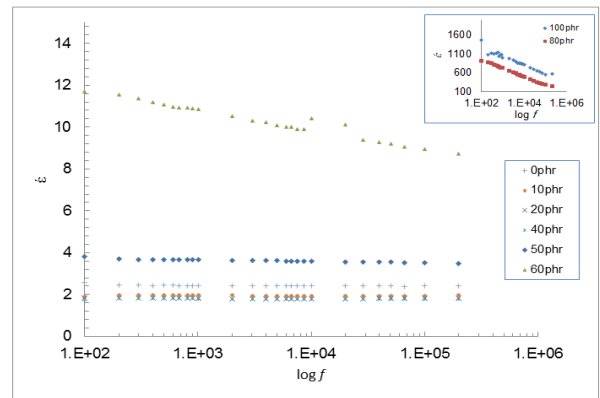


Figure (4): Frequency dependence of ϵ' of graphite/IIR composites in membrane form.

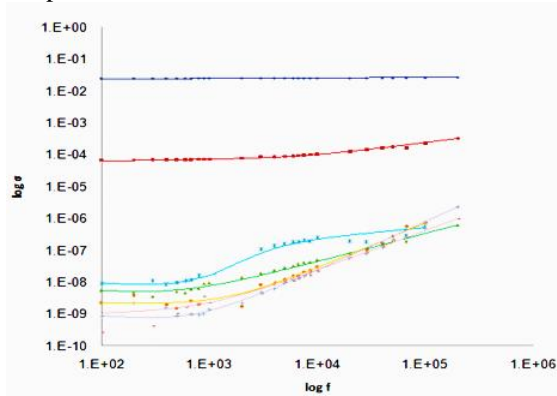


Figure (5): The frequency dependence of σ_{AC} of graphite/IIR composites in the bulk form.

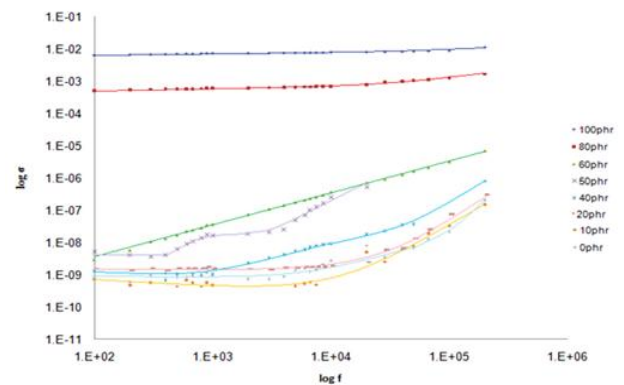
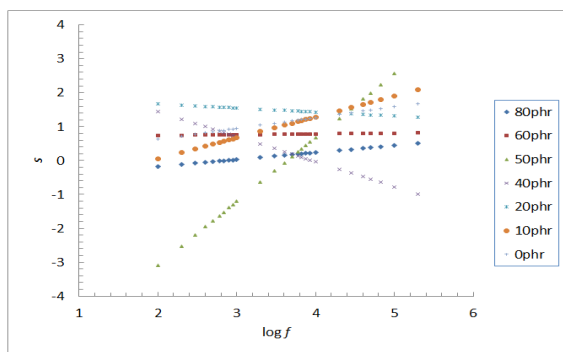
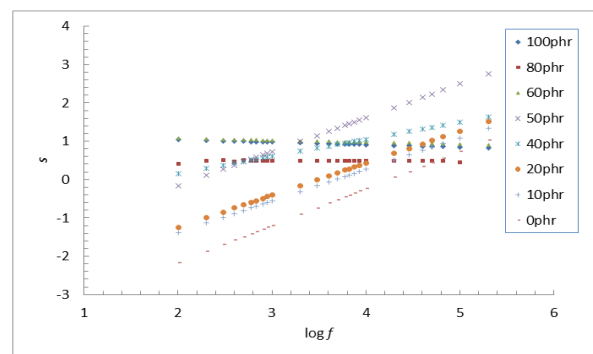


Figure (6): The frequency dependence of σ_{AC} of graphite/IIR composites in membrane form.



Figure(7): Variation of s as a function of $\log f$ for IIR bulk samples



Figure(8): Variation of s as a function of $\log f$ for IIR membrane samples

Conclusion

Using graphite powder as a reinforcing conducting filler in IIR matrix causes the dielectric constant to increase by few orders of magnitude (almost 3 orders of magnitude) upon increasing the filler loading above the percolation threshold (≈ 0.25) and frequency exponent values obtained were far from the reported values. However, that was attributed to several factors of which, the polymer filler interaction was not taken into account. Also, it was found that QMT is dominant in samples 20 phr and 40 phr in bulk form and 60 and 100 phr in membrane form, while CBH is operative in all other samples.

References

1. Pinto G., Jimenez-Martin A., *Polym. Compos.* 22(2001) 65.
2. Hepel M., *J. Electrochem. Soc.* 145 (1998) 124.
3. Flandin L., Bidan G., Brechet Y., Cavaile J.Y., *Polym. Compos.* 21(2000)165
4. Otero T.F., Cantero I., Grande H., *ElectrochimActa* 44(1999) 2053.
5. Roldughin V.I., Vysotskii V.V., *Prog. Org.Coat.* 39(2000)81.
6. Kirkpatrick S., *Rev. Mod. Phys.* 45 (1973) 574.
7. Carmona F., *Physica A* 157 (1989) 461
8. Celzard A., Mareche J.F., Furdin G., *Phys. D. Appl. Phys.* 33(2000) 3094
9. Lu W., Lin H.F., Wu D.J., *Polym.* 47 (2006) 4440.
10. Chen G.H., Wu D.J., Weng W.G., *Polym. Int.* 50 (2001) 980.
11. Chen G.H., Wu D.J., Weng W.G., *Acta. Polym.Sin.* 6 (2001) 803
12. Xiao P., Xiao M., Gong K., *Polym.* 42 (2001) 4813
13. Chen G.H., Wu D.J., Weng W.G., *J. Appl. Polym. Sci.* 82 (2001) 2506
14. Pan Y.X., Yu Z.Z., Ou Y.C., *J. Polym. Sci. Part B Polym. Phys.* 38 (2000) 1626.
15. Tchmutin I.A., Ponomarenko A.T., Efimov O.N., *Carbon* 41(2003) 1391.
16. Du X.S., Xiao M., Meng Y.Z., *Eur. Polym. J.* 40(2004)1489.
17. Chen G.H., Weng W.G., Wu D.J., *Carbon* 42 (2004) 753
18. Chen G.H., Weng W.G., Wu D.J., *Eur. Polym. J.* 39(2003)2329
19. Chen G.H., Wu D.J., Weng W.G., *Polymer* 44(2003)1781
20. Dahiya H.S., Kishore N., Mehra R.M., *J. Appl. Polym. Sci.* 106 (2007) 2101
21. Hippel A.R.V., *Dielectrics and Waves.* 1953 Wiley: New York
22. Elliott S.R., *Adv. Phys.* 36 (1987) 135
23. Gudmundesson J.T., Svavarsson H.G., S.Gudjonsson S., Gislason H.P., *Phys. B* 340 (2003) 324
24. Nan C.W., *Prog. Mater. Sci.* 37 (1993) 1
25. Balberg I., *Phys. Rev. Lett.* 59 (1987) 1305
26. Wu J., McLachlan D.S., *Phys. Rev. B* 56 (1997) 1236.
27. Kilbride B.E., Coleman J.N., Fraysse J., Fournet P., Cadek M., Drury A., Roth S., Hutzler S. B., Blau W.J.J., *J Appl. Phys.* 92 (2002) 4024.
28. Stauffer D, Aharnoy A. *Introduction to percolation theory.* 1991, London: Taylor & Francis
29. Panwar V., Sachdev V.K., Mehra R.M., *Eur. Polym. J.* 43(2007) 573.
30. Al-Shabanat M., *J. Polym. Res.* 19(2012) 9795
31. Bhattacharyya S., Saha S.K., Chakarvory M., Mandal B.M., Chakarvory D., and Goswami K., *J. Polym. Sci. part B Polym. Phys.* 39 (2001) 1935.
32. Elliott S.R., *Phil. Mag. B* 36(1977) 1291.
33. Pollak M., Geballe T.H., *Phys. Rev. B* 122(1961)1742.
34. Austin L.G., Mott N.F., *Adv. Phys.* 18(1969) 41
35. Pick G.E., *Phys. Rev. B* 6(1972) 1572.

(2013) ; <http://www.jmaterenvirosci.com>